K-4-03

Extended Abstracts of the 2020 International Conference on Solid State Devices and Materials, VIRTUAL conference, 2020, pp723-724

Structural and luminescence characteristics of trench defects in red-emitting InGaN/GaN on single-crystal GaN substrate

Takashi Tange, Taeko Matsukata, and Takumi Sannomiya

Department of Materials Science and Engineering, Tokyo Institute of Technology
Yokohama, Kanagawa, 226-8503, Japan
Phone: +81-3-6891-9306 E-mail: tange.t.aa@m.titech.ac.jp

Abstract

The light emission property of InGaN quantum wells is seriously deteriorated in the red wavelength with high indium concentration, which is accompanied by structural defects called trench defects. However, the formation mechanism of trench defects has not been fully understood. In this study, we reveal the origin of this defect by utilizing the simplest system, one consisting of a single InGaN quantum well on a single-crystal GaN substrate to extract the effect solely from indium addition. Trench defects are found to be associated with a stacking fault in the cap GaN layer right above InGaN and with an excess layer in InGaN.

1. Introduction

InGaN based laser diodes (LDs) are expected as promising candidates for next-generation solid-state light source [1][2]. The realization of RGB InGaN LDs, especially for display applications, will demonstrate the further potential of nitride light emitting devices. However, the emission property is seriously deteriorated in the red wavelength range where a high-In-content InGaN layer is required and structural defects are formed [3]. The mechanism of formation of particularly well known "trench defects" is not fully understood. In order to directly answer this question of how trench defects are formed in the InGaN layer, a single quantum well (SQW) on defect-free single-crystal GaN should be analyzed. In this study, we use this ideal structure consisting of an InGaN/GaN SQW epitaxially grown on a low-defectivity single-crystal GaN substrate. We clarify the formation mechanism of trench defects by detailed structural analysis and assess the bulk and local emission characteristics. By utilizing a single-crystal GaN substrate, it is possible to eliminate the influence of residual strain of the seed layer and TDs of the substrates, which therefore allows extraction of the effect purely of indium composition increases.

2. Experimental

The investigated samples of the InGaN/GaN SQW were grown by a metal-organic CVD technique on 2-inch c-plane GaN substrates. The SQW InGaN layer of 3 nm thickness was deposited on an undoped buffer GaN layer approximately 600 nm grown at 1200 °C and capped by a GaN layer approximately 100 nm grown at 850 °C to protect the InGaN surface. The five fabricated InGaN SQWs had different emission wavelengths depending on the indium concentration (atomic %): 15%, 24%, 28%, 30%, and 34%, which were respectively named Blue, Green, Yellow, Orange, and Red after the emission color. The emission wavelength was tuned by changing the growth temperature of the SQW layer under a constant precursor gas ratio to incorporate different amounts of indium. The growth temperatures of the InGaN layers were (Blue) 888 °C, (Green) 830 °C, (Yellow) 810 °C, (Orange) 790 °C, and (Red) 770 °C. The detailed structural analysis has been investigated by atomic force microscope (AFM), scanning electron microscope (SEM) and transmission electron microscope (TEM), and assess the bulk- and local emission characteristics using photoluminescence (PL) and cathodoluminescence (CL).

3. Result and Discussion

Figure 1 shows (a) the sample structure of the InGaN/GaN SQW and (b) the PL peak intensities summarized as functions of the emission wavelength, which were measured at 100 positions within a 2 cm × 2 cm wafer. The PL peak intensity decreased exponentially as the emission wavelength increased. In particular, the PL peak intensity of sample Red was reduced by a factor of 1/180 in comparison with that of sample Blue.

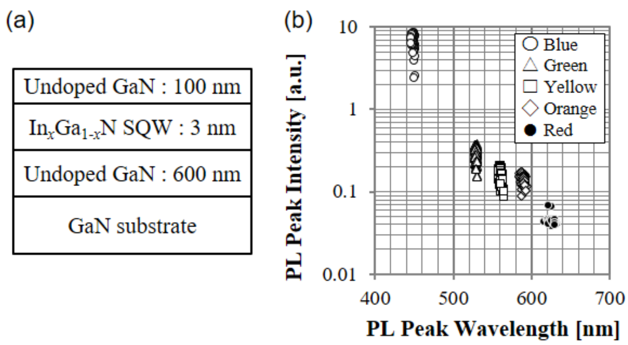

Fig. 1 (a) Structure of the fabricated InGaN/GaN SQW samples. (b) PL peak intensity [4].

Figure 2 shows AFM analysis of the sample Red. The line profile across the trench defect, as shown in Fig. 2(b), shows that the defect area encircled by a ditch was higher than the surrounding defect-free area. Since there seems some relation between the width of the trench defect [W_d defined in Fig. 2(b)] and its height [H_d, in Fig. 2(b)], we analyzed the defect height as a function of the defect width. The defect height H_d monotonically increased as the defect width increased for W_d < 100 nm while H_d decreased with a W_d increase for W_d > 100 nm [4].

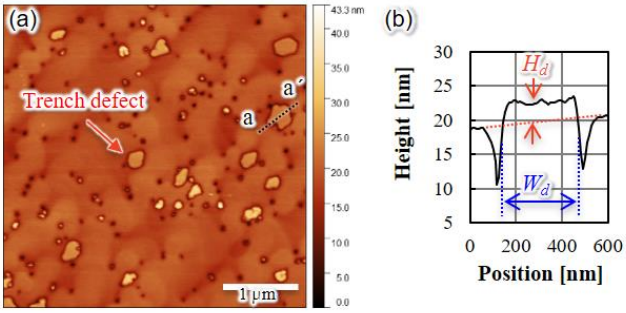

Fig. 2 (a) AFM images of sample Red. (b) AFM line profile over the trench defect of sample Red. The line profile is along the a-a′ indicated in panel (a) [4].

To obtain the precise origin of the trench defect formation, we performed TEM analysis. Figure 3 shows the results of the structural analysis by cross-section and plan-view TEM of sample Red. The cross-sectional thickness profile of the selected defect area in Figure 3(a) well agrees with the AFM profile in Fig. 2(b). As shown Fig.3(b), since the defect clearly shows almost homogeneous dark contrast inside the trench defect, the defect area must have a different crystallographic orientation. Additionally, by atomic-resolution observation, a zincblende crystal structure of A-B-C stacking in the trench defect was actually found in the cap GaN layer, located a few atomic layers above the InGaN layer [4].

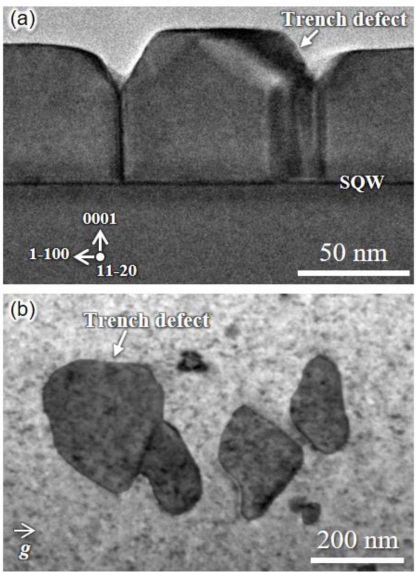

Fig. 3 (a) Cross-section and (b) Plan-view BF-STEM image of trench defect.

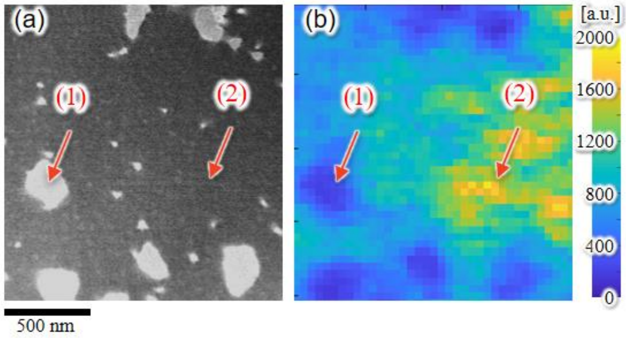

Fig. 4 STEM-CL results of sample Red. (a) ADF-STEM image of the mapped area, and (1) trench defect and (2) defect-free regions indicated by the arrows in panel (a). (b) CL mapping plots of peak intensity [4].

In order to correlate the trench defect area to the local optical property, we measured the nanoscopic emission distribution of sample Red by STEM-CL at room temperature. Figure 4(a) shows an annular dark field (ADF) STEM image of the observed area and Figure 4(b) shows the peak intensity distributions. In the peak intensity map in Fig. 4(b), the trench defects are mostly distributed in the lower emission intensity area.

4. Conclusions

By using a low-defect single-crystal GaN substrate and a single InGaN/GaN quantum well structure, we investigated the formation mechanism of trench defects. Trench defects were a cause of local emission degradation. TEM analysis indicated that the trench defects introduced a zincblende-type stacking fault in the capping GaN layer a few atomic layers above the InGaN quantum well layers to relax strain induced by the excess indium layer.

Acknowledgements

The authors thank the Suzukakedai Materials Analysis Division, Technical Department, Tokyo Institute of Technology, for the TEM measurement.

References

[1] Y. Nakatsu, Y. Nagao, K. Kozuru, T. Hirao, E. Okahisa, S. Masui, T. Yanamoto and S. Nagahama: Proc. SPIC. 10918, 109181D (2019).

[2] J.J. Wierer, J.Y. Tsao and D.S. Sizov: Laser & Photonics Reviews. 7 [6], 963(2013).

[3] S. Lutgen, D. Dini, I. Pietzonka, S. Tautz, A. Breidenassel, A. Lell, A. Avramescu, C. Eichler, T. Lermer, J. Muller, G. Bruederl, A. Gomez, U. Strauss, W.G. Scheibenzuber, U.T. Schwarz, B. Pasenow and S. Koch: Proc. SPIE. 7953, 79530G (2011).

[4] T. Tange, T. Matsukata and T. Sannomiya, Appl. Phys. Express, 13, 062004 (2020)